DESIGN OF THE LHC BEAM DUMP

A. Ferrari*, A. Ijspeert+, G. R. Stevenson+
and E. Weisse+.
* I.N.F.N., LASA Laboratory, I-20090 Segrate, Milan.
+ CERN, CH-1211 Geneva, Switzerland.

Abstract

A tentative design of the beam dumps for the Large Hadron Collider has been developed which takes account of the severe constraints imposed by the high intensity and magnetic rigidity of the beam. A spiralling beam shape at the front surface of the dump is provided by two kicker magnets operated with a 90° phase shift. However the technological constraints given by the kickers and the spatial constraints given by the tunnel construction limit the maximum achievable deflection to a few centimetres. Computer simulations of the cascade generated by the 8 TeV protons indicated the need for further dispersive mechanisms to keep the maximum temperature rise of the graphite core of the dump below the safety limit. The solution investigated here is one in which one or more graphite scatterers are interposed between the kickers and the dump. Details are given of the reduction in the maximum energy density in the dump provided by this scattering technique.

1. Introduction

Work on the design of a beam dumping system for CERN's Large Hadron Collider (LHC) [1] is progressing. In the current proposals, each of the circulating beams may contain up to 5×10^{14} protons at a maximum energy of 8 TeV, corresponding to a stored beam energy of 640 MJ. The beam dumping strategy adopted involves a fast extraction of the beam from the machine, which is then transported to an external absorber housed in an underground cave some 750 m downstream of the extraction point (Fig.1). Graphite has been chosen as the principal energy-absorbing material because of its low atomic weight (and consequent lengthening of the electromagnetic component of the cascades produced by the protons), its relatively low density (1.75 g/cm^3), which dilutes the hadronic component of the cascade, and its excellent mechanical properties which subsist at temperatures up to 2500°C. The central graphite core is surrounded by heavier materials, aluminium and iron, to obtain sufficient shielding against residual radioactivity with the minimum of lateral dimensions.

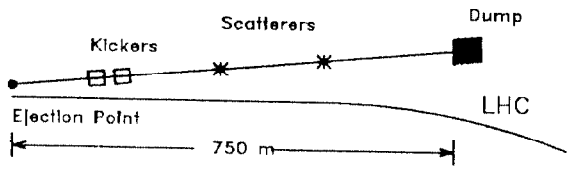

Fig. 1 Beam Transport to the External Dump

The limited transverse emittance of the LHC beam (~ 0.002 mm mrad at 8 TeV) is such that the size of the beam even after drifting over several kilometres is still so small that energy deposition densities in a graphite dump (and hence instantaneous temperature rises) are far in excess of those which can be tolerated. Therefore additional means of diluting the beam have to be found. One very efficient procedure is to deflect the beam by an orthogonal pair of kicker magnets so that the beam spirals on to the front face of the graphite absorber [2]. In the present note we discuss a different dispersive mechanism, that of placing one or several small scattering blocks in the extracted beam between the kicker magnets and the absorber. These must be of a size sufficient to diffuse the beam by nuclear elastic and multiple Coulomb scattering but must not be large enough to develop the electromagnetic and hadronic cascade significantly.

2. Description of the calculations

The FLUKA Monte-Carlo code [3] was used to simulate the development of the electromagnetic and hadronic cascades generated by the 8 TeV protons inside the dump structure. However the standard version of this code was slightly modified so that it better represented the interactions of these very high energy beams with matter. Parameters used in the hadron-hadron collision model which generates secondary hadrons at these higher energies were slightly modified so that they gave rapidity, multiplicity and transverse momentum distributions which were more in agreement with experimental data at current collider cms energies (corresponding to an energy in the Laboratory frame which is higher than the beam energy of the LHC). Parameters used in the generation of rapidity and multiplicity distributions for hadron-nucleus collisions were also tuned to new experimental data: however these data are of course available only for energies up to a few hundred GeV. Particular care was taken in matching the computed transverse momentum distributions with the experimental ones for hadron-hadron collisions, at least for transverse momenta up to 2 GeV, since this governs the beam divergence after the first interactions with the dump material. There now appears to be an excellent agreement between computed and experimental rapidity distributions and multiplicities: in particular the growth of the rapidity plateau and of the average charged particle multiplicities with energy seem to be well represented by the present version of the code [4]. Good agreement between the code and experiments for hadron-nucleus interactions at several hundred GeV and for hadron-hadron reactions at LHC primary energies is not enough to be sure that the physics represented in the FLUKA code is reliable for hadron-nucleus collisions at LHC energies, since new physical phenomena could be present (and a few are expected). However, until actual experimental data

become available from the LHC, the present simulations are the best which can be provided for inelastic collisions, provided that suitable safety factors are applied to the results to account for these uncertainties, which may amount to 30-50% if there is no "new" physics, but could be a factor of two in the worst case.

A second improvement to the FLUKA code was a revision of the parameters used to describe elastic nuclear scattering [5].

A third, major improvement to the hadronic part of the code was the introduction of a detailed treatment of the multiple Coulomb scattering of charged particles bearing in mind the importance of any scattering mechanism which could increase the divergence of the cascade. The same scattering algorithm was also introduced inside the electromagnetic package of FLUKA, originally based on EGS4 [6], since the original one was inadequate for our purposes. Details of this new algorithm are described elsewhere [7]: all its features were exploited for these calculations, including the possibility to use suitable nuclear form factors to describe the influence of the nuclear charge distribution on the scattering, which can be quite important at high energies.

In summary the parameters used to describe the physics of hadron production and scattering has been tuned and improved trying to achieve results appropriate to the current degree of knowledge.

The dump was taken to be an 800 cm long, 70 cm diameter graphite cylinder. Actually the real dump will be larger since it will include also aluminum and iron lateral shielding, however these extra regions are of no interest in the determination of energy deposition at the maximum of the cascade and so they have been omitted from the present calculations. No beam pipe was inserted between the scatterer and the dump; however it is believed that the contribution of particles reflected back by the pipe on to the dump is negligible. The calculations have been performed using zero, one and two 20 cm thick graphite scatterers placed between the extraction point and the dump. The two scatterers were positioned at distances of 280 and 140 metres from the dump. These are the longest distances which can be considered in the present configuration of the extraction tunnel geometry. The thickness of each graphite scatterer corresponds roughly to one radiation length or one-half of an inelastic interaction length for protons at the beam energy. So about 60% of the beam particles interact before the dump in the twin-scatterer configuration, resulting in a significant divergence of the emerging beam, but without giving rise to a large energy deposition since the total length is too short to fully develop the cascade.

All particles were followed in the FLUKA simulation until they fell below an energy cut-off, set at 50 MeV for all particles except photons and electron/positrons for which the cut-off was 10 MeV. The 50 MeV hadron threshold does not affect the energy deposition at region of maximum energy deposition in the cascade since this is largely dominated by the electromagnetic cascade, while the 10 MeV threshold for the latter may result in a slight overestimation of the maximum deposition. However, lower values of the e.m. cut-off are unpractical since they would require large increase in computer time for the simulation. For this same reason the leading particle biasing technique was applied to the e.m. cascade simulation which resulted in a gain in CPU time of about a factor of 3. Suitable step sizes had to be chosen to comply with the physics constraints due to the multiple scattering implementation: multiple scattering of hadrons below 10 GeV was not implemented in order to save computer time; these particles are already diffused by previous inelastic interactions and in addition they do not deposit energy in the region of interest.

Energy deposition was scored out to a radius of 30 cm both in the dump and in the scatterers in order to avoid edge problems. A coarse bin size of 0.33 x 20 cm was used for the whole dump, while a finer mesh of 0.166 x 10 cm was used in the region of maximum energy deposition (0.166 x 2 cm in the scatterers).

3. Results and Discussion

Fig. 2 shows the radial distribution of energy density at the maximum of the cascade in a graphite cylinder when there is no scatterer present (at a depth of 150 to 200 cm into the dump). The radial bin size chosen for these calculations may still underestimate the energy density along the axis of the cascade. The maximum value taken from Fig. 2

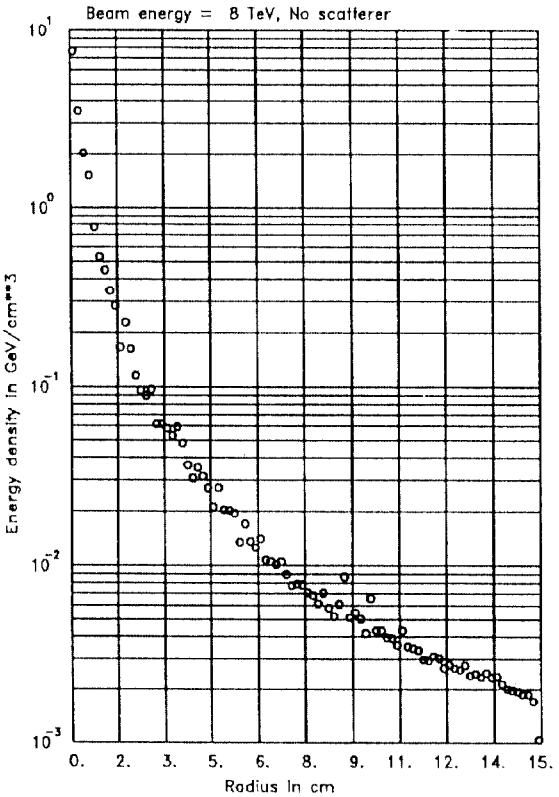

Fig. 2 Radial distribution of energy density at cascade maximum

of 8 GeV/cm^3 is some 150 times higher than could be tolerated by a graphite absorber irradiated by a beam of 5×10^{14} protons at 8 TeV.

The effect of first one and then two scatterers on this maximum energy deposition is shown in Figs. 3 and 4 respectively. One scatterer reduces this maximum by a factor of 5, while the double scatterer system gives a reduction factor of 10. This is still 15 times higher than the tolerable energy density.

By combining the scatterer and spiral kicker system one must not expect a total reduction factor which is the simple product of the reduction factors of the two systems taken separately. The beam spot "seen" by the second system will already be diffused by the first and so the second factor will not be as great as that given for an undiffused beam. Initial calculations suggest that the combined reduction factor could be high enough to give some degree of conservatism for the design of the graphite dumps.

One still has to ensure that the energy deposited in the scatterers themselves will not lead to their destruction by the beam. The FLUKA calculations suggest that the maximum energy depositions are 0.6 GeV/cm^3 for the single scatterer and 0.35 GeV/cm^3 for the second of the double scatterer system if no other beam-diffusing system were to be employed. This indicates that a spiral kicker mechanism is required to keep these energy depositions below tolerable values.

One also must investigate the disturbance on the surroundings given my the stray radiation coming from inelastic interactions of the beam in the scatterers. This will give rise to restricted areas of high dose and high induced radioactivity. However it will be possible to avoid these effects by local shielding.

References

[1] G. Brianti and K. Hubner (eds.), "The Large Hadron Collider in the LEP Tunnel", CERN 87-07, 1987.

[2] A. Ijspeert and G. R. Stevenson, "Formulae for the Calculation of Energy Deposition Densities in the Graphite Dumps of the LHC", CERN Divisional Report SPS/89-7(ABT), 1989

[3] P. A. Aarnio, A. Fasso, H. J. Moehring, J. Ranft and G. R. Stevenson, "FLUKA86 User's Guide", CERN Divisional Report TIS-RP/168, 1986.

[4] J. Ranft and A. Ferrari, Private communication, 1990.

[5] H. J. Moehring, Private communication, 1989.

[6] W. R. Nelson, H. Hirayama and D. W. O. Rogers, "The EGS4 Code System", SLAC Report SLAC-265, 1985.

[7] A. Ferrari, Private communication, 1990.

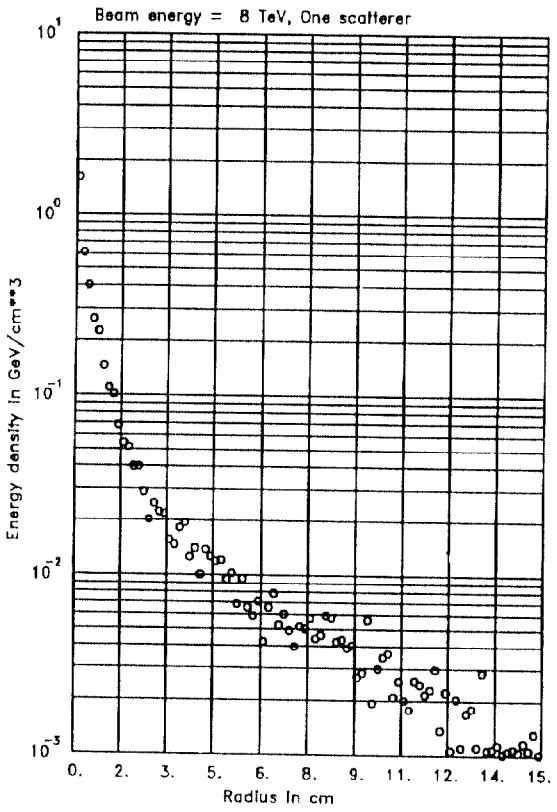

Fig. 3 Radial distribution of energy density at cascade maximum

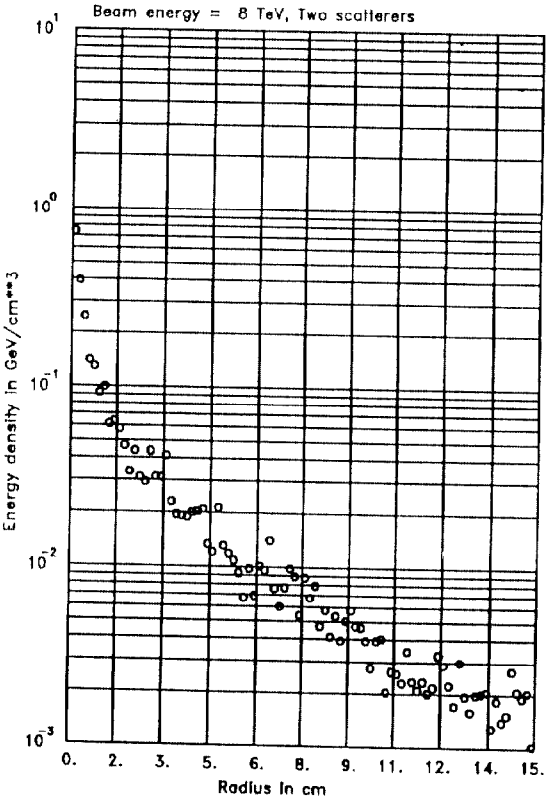

Fig. 4 Radial distribution of energy density at cascade maximum